TUDelft

Delft University of Technology

Aeroelastic tailoring of flexible composite aircraft

Natella, Mario; de Breuker, Roeland

Important note
To cite this publication, please use the final published version (if applicable).
Please check the document version above.

AEROELASTIC TAILORING OF FLEXIBLE COMPOSITE AIRCRAFT

Mario Natella[1] and Roeland De Breuker[2]

[1]PhD Candidate
Delft University of Technology
Kluyverweg 1, 2629HS, Delft, The Netherlands
marionatella@tudelft.nl

[2]Associate Professor
Delft University of Technology

Abstract: This paper presents a unified framework for aeroelastic tailoring of fully-flexible free-flying composite aircraft. A continuous-time state-space model is used to describe the flow. The 3D composite wing structure is condensed into a Timoshenko beam model utilizing a cross-sectional modeler. The aerodynamic and structural models are tightly coupled with the longitudinal flight dynamic equations of motion in the state-space formulation. This paper refers to the clamped-wing aeroelastic tailoring as classic aeroelastic tailoring. Hence, the term aeroelastic tailoring will point at the novel approach that models the flexible, free-flying composite aircraft. With this paper, the author investigates the effects on the tailored structural design in terms of optimum mass and stiffness distribution due to the flexibility of the composite aircraft.

1 INTRODUCTION

The promise of aeroelastic tailoring was to develop a design framework that could enhance aircraft structural performance at large. The idea sees great recognition in the research community in the 1980s with important works by Shirk et al. [1] and Weisshaar et al. [2], and recent developments by Stanford et al. [3], and Stodiek et al. [4]. State-of-the-art aeroelastic tailoring practices have developed frameworks to solve the problem at a wing level. The results in terms of weight saving, load alleviation and/or range optimization are very promising, thus justifying the further development in this field.

The early studies (Shirk et al. [1], Weisshaar et al. [2]) explored the potential of aeroelastic tailoring using a single fiber angle, thus describing most of the fundamental phenomena observed in composite wings and how to prevent them by inducing a beneficial bend-twist coupling. For example, a divergence critical wing (i.e. swept forward) benefits from wash-out tailoring where the bend-twist coupling is designed such that a node-down twist is induced upon bending, Weisshaar et al. [2].

In the late 1990s, aeroelastic tailoring research started to focus on laminates with different fiber angles through the thickness, an approach that increased the level of complexity of the models to describe more realistic composite structures. There are three main approaches to this problem found in literature, namely using *(i)* laminates with a fixed thickness, but varying fiber

angles, *(ii)* laminates with a fixed set of fiber angles, and varying thickness and *(iii)* laminates with both varying fiber angles and varying thickness. The first approach, where the thickness is kept constant, has been solved with evolutionary algorithms (Georgiou et al. [5], Manan et al. [6], Guo et al. [7]) or fiber steering (Haddadpour et al. [8], Stodieck et al. [4], Stanford et al. [3]) to maximize flutter speed. Both approaches already show significant improvements in overall aeroelastic performance due to varying stiffness along the span of the wing compared to the classic approach with straight fibers. The second approach, with a fixed set of discrete ply angles, provides a solution to comply with certification requirements, reduce the number of design variables (Eastep et al., Kim et al, Tian et al.) and improve aeroelastic performance under a different set of constraints including buckling, strains and aileron effectiveness.

The aeroelastic framework developed by De Breuker et al. [9] focuses on the third approach where both fiber angles and thickness are modeled as design variables to explore the full potential of aeroelastic tailoring and simplify the formulation of the optimization problem. In contrast to working with fiber angles directly, the formulation where both thickness and fiber angles are varying can be described in the continuous domain using lamination parameters thus making this problem fit for gradient-based solvers and optimization frameworks. The first description in lamination parameters was introduced by Kameyama et al. [10]. The approach was first proved for a flat composite panel, where the set of lamination parameters and thickness was calculated for maximum flutter speed. The work of Jin et al. [11], and Dillinger et al. [14] has scaled this approach to solve a similar problem for the whole wing, modeled as a multitude of chordwise and spanwise panels for a more detailed description of a composite wingbox and its structural elements.

In view of a more complete analysis, it is important to understand the classic aeroelastic phenomena in the context of the whole aircraft, in particular with respect to the interaction of the wing with fuselage and tails. The first problem encompasses the solution to the flow around the full aircraft configuration, in particular in the area near the wing-body junction. A very extensive explanation of the fuselage aerodynamics, including the effects of the wing-body interaction and its importance is found in the work of Singh et al. [16]. The main contributions of the fuselage aerodynamics are a large pitching moment and a destabilizing neutral point shift upstream. A minor contribution is the increase of effective angle of attack at the root of the wing. The lift generated by the fuselage itself is negligible. Further details regarding the interaction phenomena in a full aircraft configuration are found in the work of Rusak et al. [17]. Another important point to discuss is the vortex shedding of the body. According to Rusak et al. [17], although there is no comprehensive model to describe the phenomenon, experimental evidence shows how the effect of the body wake on the longitudinal aerodynamic coefficient is of orders of magnitude smaller, thus negligible.

To summarize, the advancement in low- and medium-fidelity physical models for the description of the aeroelastic framework have made new solutions available at the preliminary design level. Already in the early phases of the design process, it is possible to develop a framework for analysis and optmization which is capable to select an improved design candidate for the more detailed phases ahead. Certification aspects and manufacturability constraints are also important parts of the problem that can be incorporated at this level. The benefit of the low-fidelity approach is in the capability of exploring a wide range of the design space at a relatively small computational effort or cost. A preliminary study of this size would be almost unfeasible with any 2D or 3D finite element description.

Table 1: Details of constraint limits and margins of safety.

Minimum Thickness	0.00183 [m] (10 plies)
Maximum Tensile Strain	6420 [μs]
Maximum Compression Strain	4857 [μs]
Maximum Shear Strain	5332 [μs]
MS for Aeroelastic Stability	0.15
Interval of Local Angle of Attack	± 15 [deg]
MS of Buckling Factor	0.4375
Minimum Aileron Effectiveness	0.10

The aim of this paper is to build on the state-of-the-art aeroelastic framework developed at Delft University of Technology by De Breuker et al. [9] and explore the effects of the flexibility of a composite aircraft model on the tailored design in terms of optimum mass, stiffness distribution and overall aeroelastic performance, e.g. stability and maneuver load alleviation.

2 AEROELASTIC TAILORING FRAMEWORK

This work builds upon the aeroelastic framework (PROTEUS) developed at Delft University of Technology initiated by De Breuker et al. [9]. The framework serves as an analysis and optimization tool for the preliminary design of composite wings. The flow is described by means of a continuous-time state-space model, as extensively described in the work of Werter et al. [21]. The three-dimensional composite wing structure is idealized by a Timoshenko beam by means of a cross-sectional modeler.

The function of the cross-sectional modeler is twofold. First, it is used to calculate the equivalent one-dimensional beam properties starting from the three-dimensional wing model. This is done by means of a thin-walled cross-sectional modeler that was developed based on the work by Willaert et al. [22] and Ferede et al. [23]. The cross-section is discretized in linear Hermitian beam elements having constant properties and can be any arbitrary open or closed, thin-walled, composite cross-section. Using a variational asymptotic approach, the Timoshenko cross-sectional stiffness and mass properties can be determined. The second function of the cross-sectional modeler is strain recovery. This process converts the one-dimensional beam strains into surface strains. These surface strains include both the Euler-Bernoulli strains and the second-order free warping solution. The strain field is then used in the assessment of the material failure by means of the failure envelope derived by Ijsselmuiden et al. [12]. The main challenge during the optimization is that the classic composite strength failure criteria cannot be used since the stacking sequence of the laminates is unknown. The failure enveloped is a Tsai-Wu based criterion that ensures no failure regardless of the ply angle. The derivation of the failure envelope criterion as a function of the principal strains is found in Khani et al. [13].

The surface strains are also used to calculate the buckling solution and the buckling index. In a conventional wing-box structure, the buckling panels are defined as the area between two stringers and two ribs. Structural stability is thus assessed in a local sense. Stringers and ribs are assumed to be stiff enough to prevent global buckling. The analytical model is based on the work of Dillinger et al. [15], where the individual panels are assumed to be flat and the bending displacement solution is approximated with two-dimensional shape functions obtained from Lobatto (bubble) polynomials.

The aerodynamic and structural models are closely coupled into a unified framework for analysis and optimization. More details regarding the framework and its functionalities are found in the work of Werter et al. [24, 25]. The coupling of the aeroelastic and flight dynamic equations of motion is addressed in details in [30], previous published work of the author. Finally, the analytical formulation of the buckling and aileron effectiveness constraint is extensively discussed in De Breuker et al. [26].

The structural optimization via aeroelastic tailoring is performed by means of the globally convergent method of moving asymptotes (GCMMA) as presented by Svanberg [31]. The objective of the optimization is minimizing the combined structural mass of the composite wing and tail by optimizing their thickness and stiffness distribution, described as a function of lamination parameters, a formulation that is suitable for gradient-based optimizers. The constraints adopted for the aeroelastic tailoring optimization and their relative margins of safety (MS) or limits are summarized in Tab. 2. The margins of safety combine both certification aspects (according to CS25) and knockdown factors, with reference to the work of Kassapoglou [27]

3 OPTIMIZATION SET-UP AND CONSTRAINTS

In this section the classic approach to aeroelastic tailoring, namely the optimization of the clamped-free wing, will be compared to *(i)* the optimization of the free-free wing and *(ii)* the optimization of the flexible aircraft. The comparison will be discussed in terms of optimum design and its performance (e.g. structural mass, active constraints, load alleviation etc.). In this comparison we will discuss and monitor the overall mass and load (re)distribution during the aeroelastic tailoring optimization. Both distributions contribute to the final objective (structural mass) and the performance of the design.

The goal of this section is to benchmark the optimization of the free-free wing and the flexible aircraft against the classic approach to aeroelastic tailoring. We will assess the weight-saving potential, the sizing constraints in each case and the most important phenomena captured in the three approaches.

3.1 Objective and Constraints

The objective of the optimizations is to minimize the structural mass of the composite wing by optimizing its thickness and stiffness distribution, described as a function of lamination parameters. The formulation in terms of lamination parameters is continuous and is suitable for gradient-based optimizers. The present work uses the globally convergent method of moving asymptotes (GCMMA) as presented by Svanberg [31].

The constraints adopted for the aeroelastic tailoring optimization and their relative margins of safety (MS) or limits are summarized in Tab. 2. The margins of safety combine both certification aspects (according to CS25) and knockdown factors, with reference to the work of Kassapoglou [27].

3.2 Optimization Set-Up

The aircraft model used for the aeroelastic tailoring studies hereby discussed is based on the NASA Common Research Model (CRM)[1]. The geometric description of the aircraft is shown in Fig. 1, where the engine and main landing gear location are indicated. The fuel distribution is instead given in Fig. 2. The load cases adopted for the study can be found in Tab. 3.

Table 2: Details of constraint limits and margins of safety.

Minimum Thickness	0.00183 [m] (10 plies)
Maximum Tensile Strain	6420 [μs]
Maximum Compression Strain	4857 [μs]
Maximum Shear Strain	5332 [μs]
MS for Aeroelastic Stability	0.15
Interval of Local Angle of Attack	±15 [deg]
MS of Buckling Factor	0.4375
Minimum Aileron Effectiveness	0.10
Phugoid Damping	≥ 0.04
Flight Path Angle	≤ 0.06
Short-Period Damping (CAT. B)	$0.30 \leq \zeta \leq 2.00$

Table 3: Overview of static load cases.

LC	Mach [-]	EAS [m/s]	n_z	Description
1	0.85	240.0	2.5	Pull-up maneuver
2	0.60	198.0	-1	Push-down maneuver
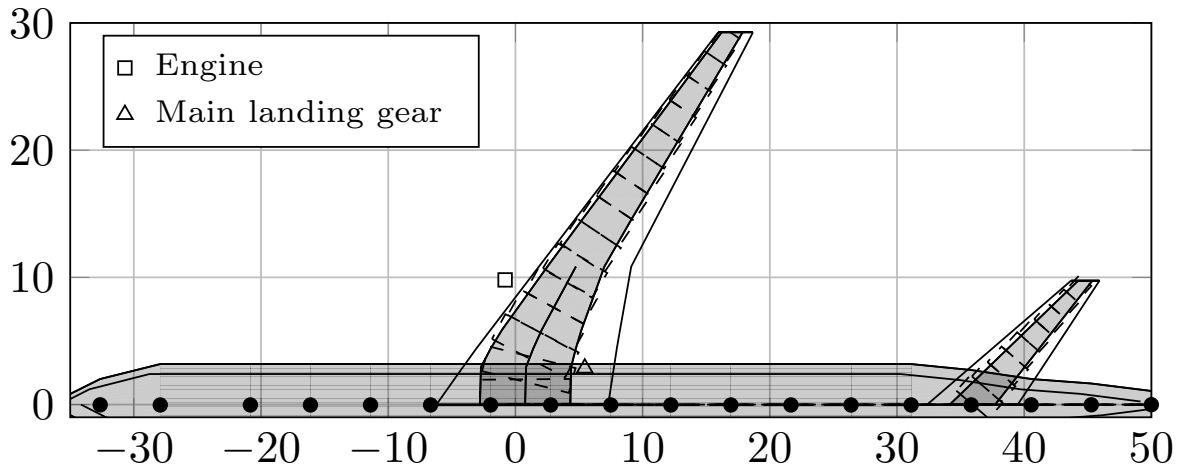
Figure 1: CRM aircraft model. Length in SI unit [m].
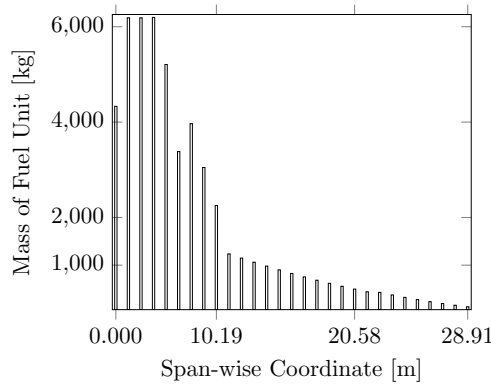*Note: only the wing and horizontal tail are optimized (optimization ID = 2).*

Figure 2: Fuel distribution along the wing.

At the start of the optimization the wing has a zero-dominated layup (60% in 0, 10% in 90 and 30% in ±45) for top and bottom skin and quasi-isotropic (QI) spars. Such stiffness distribution is widely used as a reference in aeroelastic tailoring, as discussed in Dillinger et al. [15], for a more realistic estimation of the weight-saving potential of aeroelastic tailoring as opposed to a QI initial design which is highly over-designed. The fuselage, in the flexible aircraft case with an initial mass of 21800 kg, has a QI stiffness distribution and both stiffness and thickness are kept constant throughout the optimization.

Three aeroelastic tailoring optimizations have been run on the CRM-wing model: *(i)* the classic aeroelastic tailoring optimization with a clamp-free wing (ID = 0), *(ii)* the aeroelastic tailoring of a free-free wing (ID = 1) and *(iii)* the flexible aircraft model (ID = 2). The design variables for each of the three optimizations are the lamination parameters and the thickness of the composite wing, and the ones of the horizontal tail for the flexible aircraft case. The goal of the study is to observe the difference in optimum design due to mass and load (re)distribution. This shift is the main cause of the difference in the sizing constraints. The specific loading condition and mass distribution influence the severity of a particular constraint, which translates into an influence in the design space available to the optimizer to look for optimum solutions.

Below follows an overview of the optimization set-up for all three cases addressed in this chapter, together with a visual representation of the differences between the three optimizations.

		ID 0	ID 1	ID 2
Model Details	Wing is optimized.	✓	✓	✓
	Tail is optimized.			✓
	Fuselage flexibility.			✓
	Fuselage is optimized.			
Constraints	Buckling	✓	✓	✓
	Material Failure	✓	✓	✓
	Aeroelastic Stability	✓	✓	✓
	Flight Dynamics Stability		✓	✓

---

[1]https://commonresearchmodel.larc.nasa.gov

6
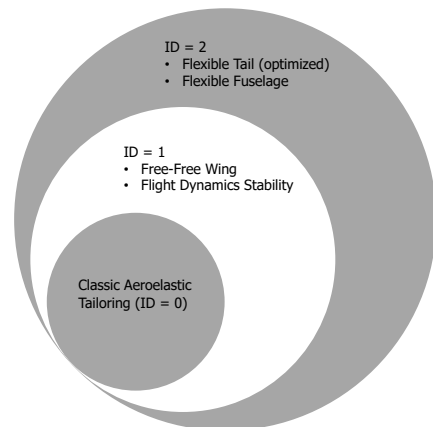
Table 4: Converged objective in comparison. Wing structural mass is indicated.

ID	Model	mass [kg]	Δ [%]
0	Clamped-Free Wing	4650	N/A
1	Free-Free Wing	4846	+4.4
2	Flexible Aircraft	5215	+12.0

4 OPTIMIZATION RESULTS

The wing-only optimization (ID = 0) converged to a final structural mass[2] of 4650 kg, which will be used as a reference for this discussion. As shown in Tab. 4, the free-free wing (ID = 1) has a structural mass of 4846 kg (about 4.4% heavier), whereas the aircraft (ID = 2) shows an increase in the structural mass of approximately 12% to about 5125 kg. These results can be explained by looking at the physics behind aeroelastic tailoring, and some of the results shown in the appendix.

In short, there is several main physical factors that are driving the results of these optimizations, namely *(i)* the severity of the handling quality constraints in optimization 1, and *(ii)* the beneficial effect of the horizontal tail flexibility in optimization 2, *(iii)* its detrimental effect in optimization 2, and *(iv)* the tailoring effects resulting from a change in mass and fiber angle distribution.

4.1 Influence of the handling quality constraints

In optimization 1 we are designing a free-free wing via aeroelastic tailoring requiring a stable *Level 1* design (in terms of handling qualities). This constraint implies that *1)* the design shows no dynamic instability and *2)* the modal response falls within a prescribed interval of frequency and damping. Among the four main responses monitored for the assessment of the longitudinal handling qualities (short period frequency and damping, phugoid damping and flight path), the short-period is the most critical since the process of aeroelastic tailoring tends to destabilize it as a consequence of load redistribution during the optimization.

In particular, the objective of aeroelastic tailoring is weight minimization which implies a wing root bending moment minimization (RBM) by moving lift inboard. For a swept-back wing, an inboard movement of the lift vector also implies a forward movement (towards the aircraft nose). At the same time, the center of gravity (CG) is also moving backwards (towards the rear of the aircraft) due to the fact that the wing weight decreases during the optimization. These two factors cause the aerodynamic center (AC) moves in front of the CG, which indicates an unstable short period mode. An example of a design with an unstable short-period as a result of an aeroelastic tailoring optimization process is found in previous work of the author in [30]. In this case the author only monitored the short-period response to observing its evolution during a tailoring optimization.

Enforcing handling quality constraint means not only correcting this tendency to instability but also steering the short-period response into a prescribed range. Moreover, steering the short-period response into a certain range (for example Level 1) has to do with increasing the frequency separation between short-period and first out-of-plane bending. Since these two modes fall in a similar range of frequency (1-5 Hz), these modes can resonate thus leading to body-freedom instabilities. A clear frequency separation can already be seen in stiff wing models (for

---

[2]The structural mass includes the mass of skins, spars, and stringers.
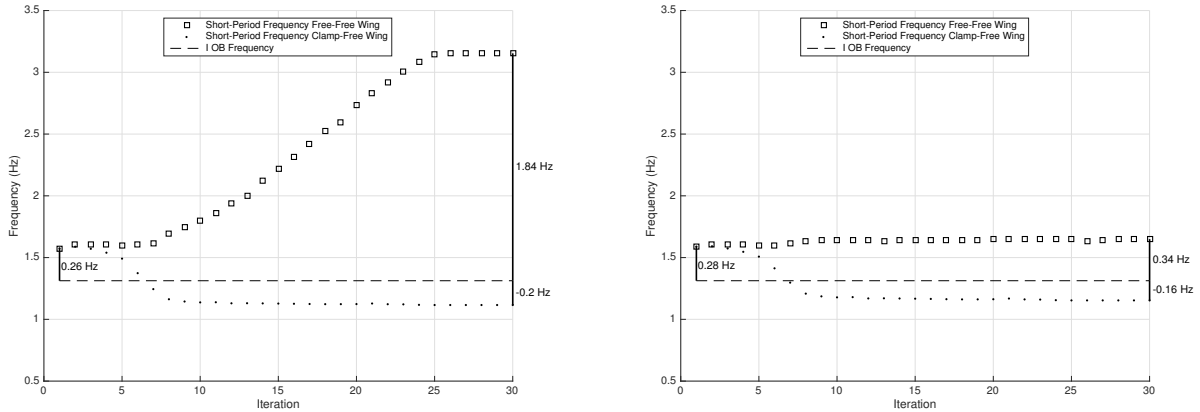
(a) Load case 1 (pull-up maneuver)　　　　　(b) Load case 2 (push-down maneuver)

Figure 3: History of short-period and first out-of-plane bending (IOB) frequencies.

example, conventional aluminum wings), but as the structures increase in flexibility the relative difference becomes less. The value of the two frequencies has been monitored during the optimization for both the clamped-free wing (where the constraint is not applied) and the free-free wing. The history is shown in Fig. 3 for both loads cases. For the optimum design the Level 1 value for the short-period frequency is of 1.87 Hz. The value of the short-period frequency at the end of the optimization is 3.15 Hz, with a separation of 1.84 Hz from the first out-of-plane bending mode (that is at 1.31 Hz). We can now also better understand and quantify the significance of the handling quality constraint prescribed by the regulations. With a minimum frequency of 1.87 Hz to be achieved, the authorities are enforcing a frequency separation of at least 0.5 Hz. Finally, note how the clamped-free wing would violate this condition, reaching a frequency separation of only 0.2 Hz at the end of the optimization.

In synthesis.

- The load redistribution that occurs during the process of an aeroelastic tailoring optimization tends to destabilize the short-period repose (which is one of the handling quality constraints enforced on the design).
- This tendency can be corrected thus obtaining a stable *Level 1* design in terms of handling quality. This correction results in an increase in structural mass of the optimum design.
- The handling quality constraint prescribed by the authorities means requiring a minimum separation frequency between the short-period and the first out-of-plane bending frequency.

4.2 Beneficial effect of the flexible tail

In the previous subsection (1.3.1 *Influence of The Handling Quality Constraints*) we discussed how the aerodynamic center (AC) and center of gravity (CG) move during an aeroelastic tailoring optimization as a result of the load redistribution caused by stiffness and mass tailoring. The relative position of the CG with respect to AC is important for the stability of the aircraft in flight. One of the reasons as to why the handling quality constraints have heavy consequences for the optimum design in terms of final structural mass is because it becomes difficult to correct the short-period response when the optimizer has a narrow range of available CG positions. In optimization 1 (free-free wing), the only parameter to vary the CG position is the wing structural mass distribution, but the range is rather narrow compared to optimization 2 (flexible aircraft) where the optimizer can vary the mass of the horizontal tail as well. Changing the mass dis-

tribution on the horizontal tail has a bigger effect on the CG position because of the relative distance between the two surfaces (i.e. wing and horizontal tail.). This is what we refer to as the *beneficial* effect of the tail.

To put things into perspective. In optimization 1 the maximum difference in terms of CG between the first and last iteration of the optimization is 1.80 m, compared to a shift of 3.41 m in optimization 2. The wider range of CG position is a favorable tool, in unison with the stiffness and mass tailoring, to correct the short-period response. This statement is also supported by the fact that the flight dynamic stability is not active in optimization 2. The sizing constraint in this case is a combination of material and buckling failure.

4.3 Detrimental effect of the flexible tail

The terms *detrimental* refers to the fact that a certain behaviour causes the objective function (to minimize) to increase in value. The detrimental effect of the horizontal tail is due to the fact that it has the potential to increase the loading conditions on the wing, thus increasing the stress and the severity of buckling on the wing surface. The magnitude of the loads experienced by the tail is relatively low compared to the ones on the wing so that the condition on the tail is not critical.

The influence of the tail is particularly on the moment equilibrium and it depends on the relative position between the wing aerodynamic center (AC) and the aircraft center of gravity (CG).

In case the CG is in front of the AC, the horizontal tail generates negative lift to balance the moment. As a result, the lift the wing has to generate is equal to the weight plus the lift generated by the tail,

$$L_{\text{wing}} = W + L_{\text{tail}} \tag{1}$$

hence

$$L_{\text{wing}} > W \tag{2}$$

The opposite scenario, where the AC is in front of the CG, the horizontal tail generates positive lift, thus,

$$L_{\text{wing}} < W \tag{3}$$

In synthesis:

- The horizontal tail has the beneficial effect of extending the range of available CG position to correct the flight dynamic stability.
- The horizontal tail has the detrimental effect of increasing the loading conditions (depending on the relative position of AC and CG) on the wing, thus increasing the strain levels.
- The job of the optimizer is to find the appropriate balance between moving the AC (through load redistribution) and moving the CG (through mass redistribution) to achieve *1)* optimal stability and *2)* manageable stress/strain levels.

4.4 Overview of the "forces" behind the optimization

With the term *forces* the author refers to the set of factors that drive the objective function to its minimum value. The adjective *beneficial* will be used to indicate that any particular factor/event tends to decrease the objective function (directly beneficial) or create a certain condition that is

favorable to a decrease in objective function (indirectly beneficial - e.g. a decrease in the strain level leads to a lighter design because the wing is under less critical loading conditions). Vice versa, *detrimental* will refer to those factors/events causing, directly or indirectly, an increase in the objective function.

Beneficial Forces.

- Decrease in root-bending moment due to an in-board shift of the lift distribution.
- Decrease in overall lift due to the positive lift generated by the horizontal tail (NB: this also implies that the AC is in front of the CG).
- Wide range of CG positions available and attainable through mass redistribution by the optimizer.

Detrimental Forces.

- AC moves in front of the CG due to an in-board shift of the lift distribution.
- Increase in overall lift due to the negative lift generated by the horizontal tail (NB: this also implies that the CG is in front of the AC).
- Narrow range of CG positions available and attainable through mass redistribution by the optimizer.

It is important to mention how some of the forces behind the optimization are at odds with each other, with the same force having the potential of being both beneficial or detrimental depending on the particular case. For example, a shift in the relative position of AC and CG can either cause a decrease in root-bending moment (beneficial) or a dynamic instability (detrimental) depending on the circumstances and the severity of the other constraints (which also steer the load distribution in a certain direction).

Here is the job of the optimizer, through the sensitivities, to find the path with the least conflict between these forces and achieve an optimal objective. We have also seen how the optimizer, as a last resort, makes use of a classic approach to solving some of the design and stability requirement, namely increasing the structural mass. By increasing the mass, and the rigidity of the structure, does two things to the design: *1)* it automatically increases the frequency separation between flexible and rigid modes (because of the decrease in flexibility), *2)* it decreases the overall stress levels of the structure.

A visual overview of the forces is shown below in Fig. 4.

4.5 Stiffness and Mass Tailoring

The results on stiffness and thickness tailoring are summarized in Appendix 5. In all three optimization cases, we can see the following trends,

- a beneficial wash-out effect is induced by controlling the stiffness and thickness distribution. An example of wash-out control through material tailoring is observed in the spar thickness distribution in Appendix A where the front spar is thicker than the rear spar. This allows the rear spar to deform more, compared to the front spar, and thus reduce the local angle of attack. A similar trend can be seen in the top and bottom skin in chord-wise direction. The stiffness tailoring, on the other hand, controls the local twist distribution by rotating the principal direction of the design patches. This phenomenon can be observed in the optimized stiffness distribution of both top and bottom skin in Appendix B and C.,
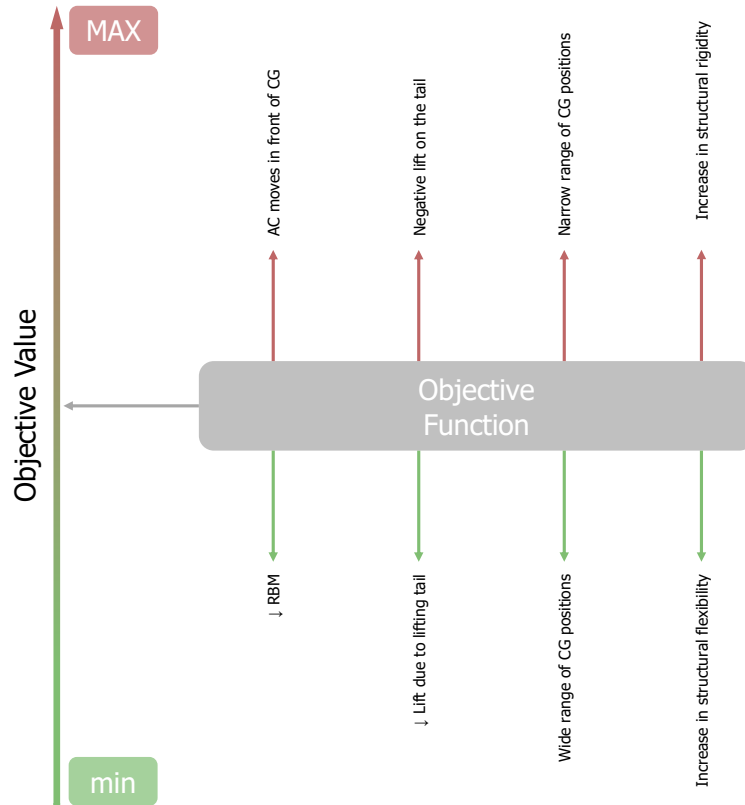
Figure 4: Visual overview of the "forces" behind the optimization.

- the optimized stiffness distribution is a result of the particular active constraint associated with every patch. For example, the patches where the buckling failure index is closer to the critical value of 1.0, the optimized stiffness approaches almost a cross-ply stiffness distribution that is most suitable for a buckling driven design. On the other hand, a very defined principal direction is typical of patches where the strain failure index is critical.

4.6 Margins

This paragraph discusses the results in terms of margins calculated during the optimization via aeroelastic tailoring. An overview of the strain and buckling failure indexes of the design configurations used for this study is shown in Appendix C. Both measures are conservative to account for material imperfections, damage and scatter.

The strain and buckling failure indexes are active in maneuver load cases. The failure indexes are influenced by the internal load distribution, and consequently both the material and stiffness distribution of the optimized design will determine whether strain or buckling failure occurs first. In particular:

- in optimization 1, due to load redistribution for both load alleviation and to stabilize the handling quality response, the inboard area are under high loading conditions causing both strains and buckling indexes to reach the prescribed margin.
- in optimization 2, the wing is sized by a combination of buckling and strain. The strain levels are relatively higher compared to optimization 0 since the horizontal tail has a detrimental effect generating opposite lift to balance out the moment. This happens because the CG is pushed in front of the AC to stabilize the aeroelastic system.

11

5 CONCLUSIONS

In this paper we have benchmarked the aeroelastic tailoring optimization of the composite aircraft against the classic approach to aeroelastic tailoring. The framework developed at Delft University of Technology for classic aeroelastic tailoring for wing structures has been extended to be able to model the flexibility, flight dynamics and aeroelasticity of the aircraft structures, [30]. While the optimum design in the reference case (classic aeroelastic tailoring) is driven primarily by material failure and/or buckling margins, there is additional factors that play an important role when optimizing the aircraft structure. The maneuverability constraints are easier to satisfy for the aircraft structure given the wider range of variation of the center of gravity (CG) position that can be achieved by controlling the mass distribution of both wing and horizontal tail. This generally means that the CG is kept in front of the aerodynamic center. This is however not a favorable condition in terms of overall stress conditions for the wing. In this case the horizontal tail generates negative lift, and as a consequence the wing experiences higher loads. This increase in the loading conditions causes an increase in the objective function and consequently an increase of the structural mass of the optimum design. The increase benchmarked against the reference case is about 12%. Parallel to these two optimizations we have also looked a second case where the free-free wing has been optimized, taking into account the flight stability and maneuverability. The additional structural mass needed to stabilize this response passively is about 4.5%. It is important to note how the variation of the loading condition during aeroelastic tailoring inevitably changes the loading conditions experienced by the horizontal tail, reason why it is worthwhile including it in the optimization loop.
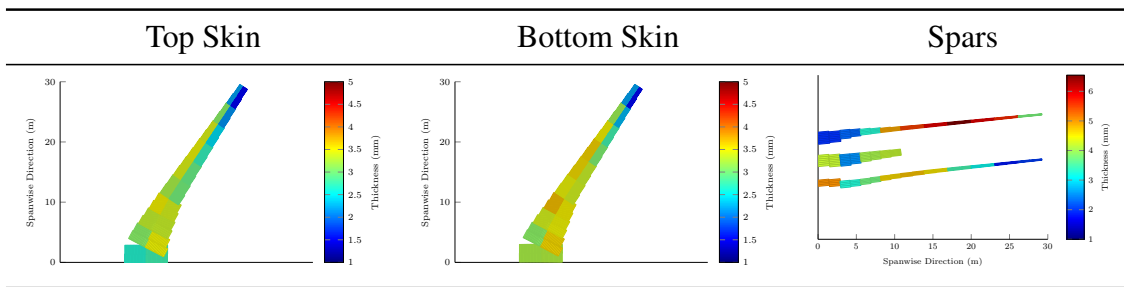
A THICKNESS

Figure 5: Optimized thickness of the reference wing (ID = 0).
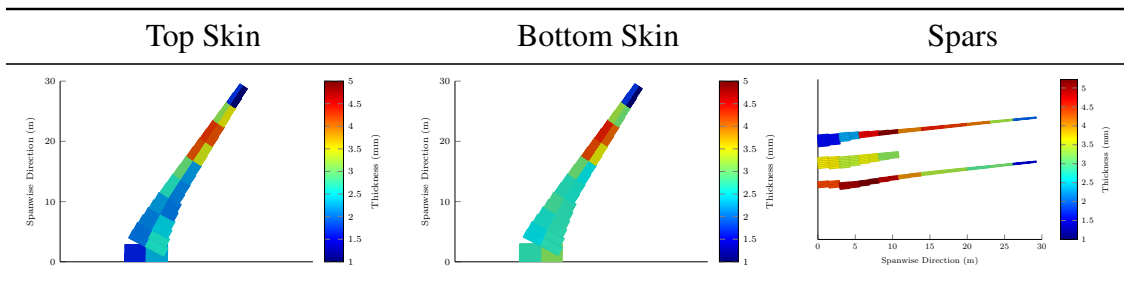

Figure 6: Optimized thickness of the free-free wing (ID = 1).
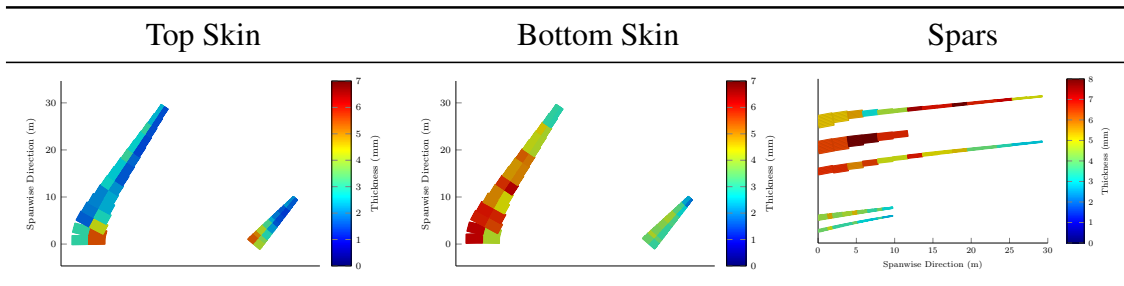

Figure 7: Optimized thickness of the flexible aircraft (ID = 2).
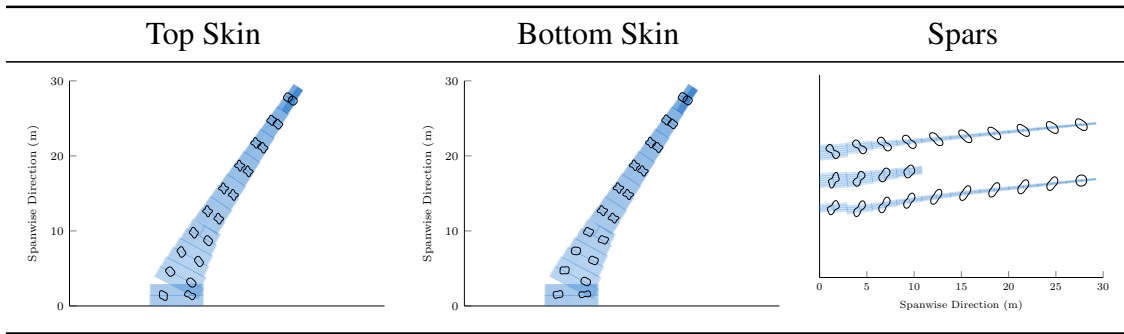
B IN-PLANE STIFFNESS

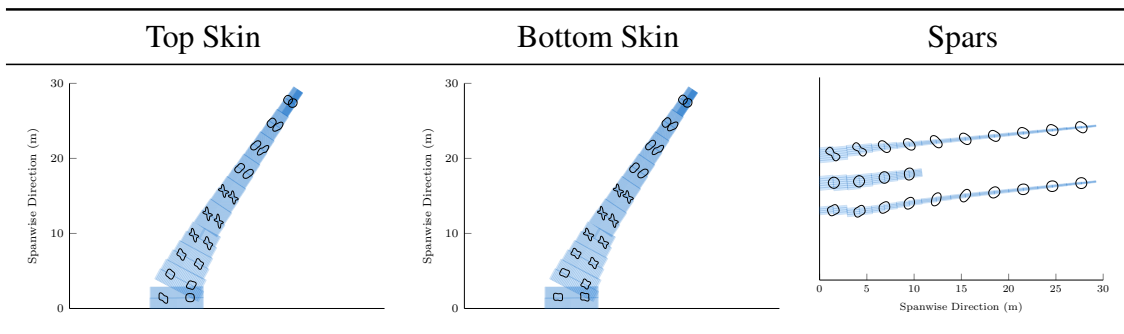Figure 8: Optimized in-plane stiffness of the reference wing (ID = 0).

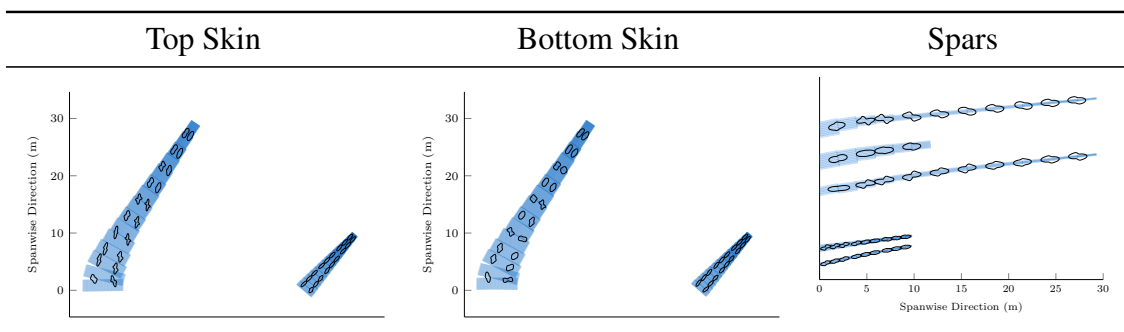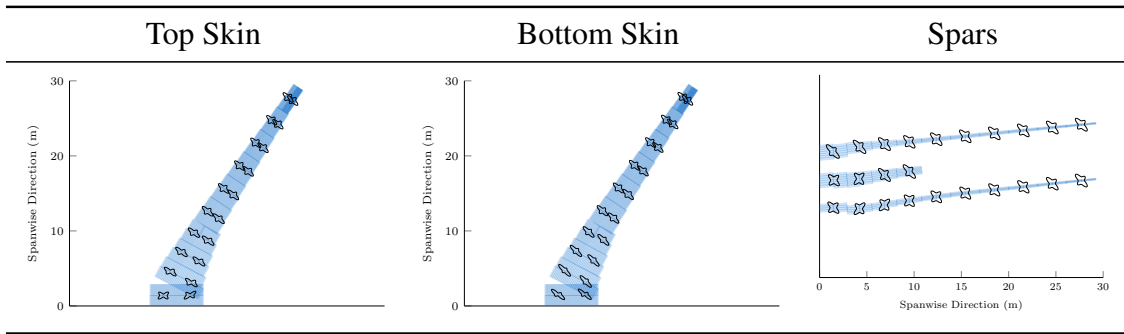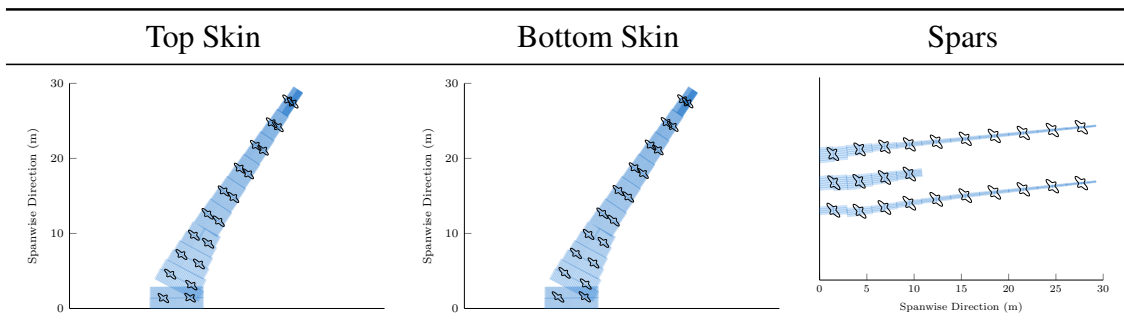Figure 9: Optimized in-plane stiffness of the free-free wing (ID = 1).

Figure 10: Optimized in-plane stiffness of the flexible aircraft (ID = 2).

C OUT-OF-PLANE STIFFNESS

Figure 11: Optimized out-of-plane stiffness of the reference wing (ID = 0).

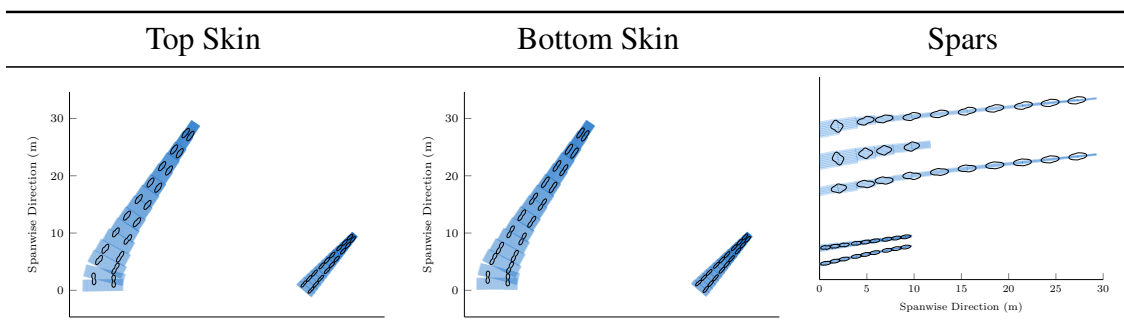Figure 12: Optimized out-of-plane stiffness of the free-free wing (ID = 1).

Figure 13: Optimized out-of-plane stiffness of the flexible aircraft (ID = 2).
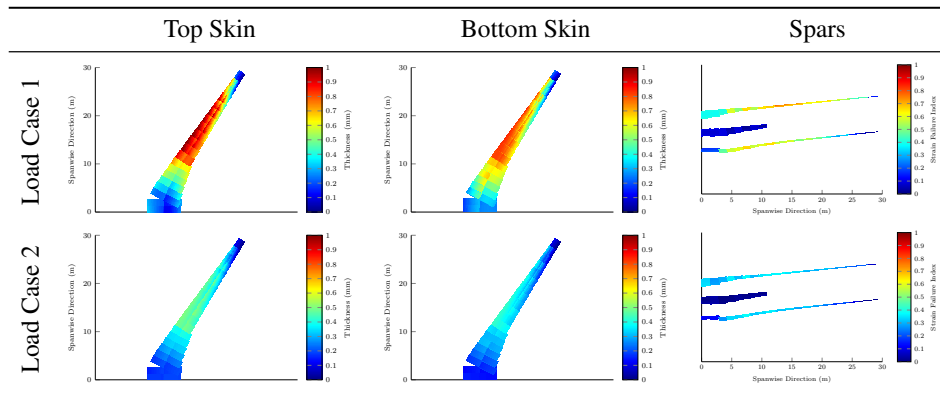
D STRAIN FAILURE INDEX

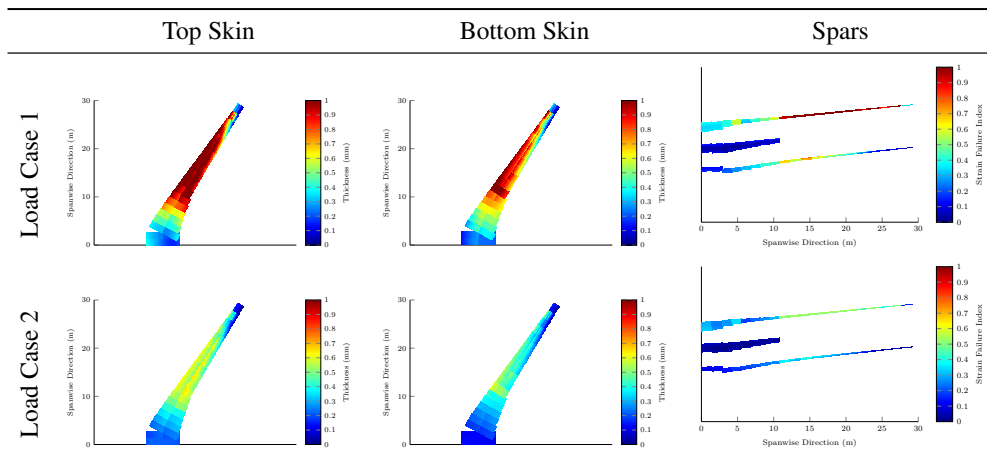Figure 14: Strain failure index of the reference wing (ID = 0).

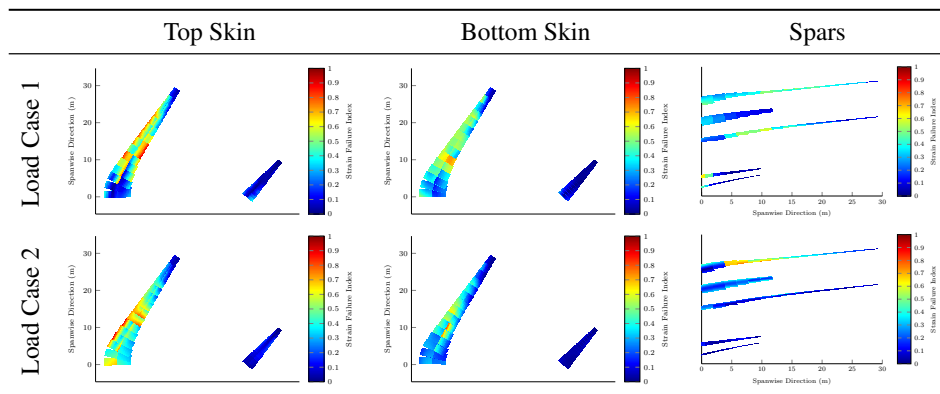Figure 15: Strain failure index of the free-free wing (ID = 1).

Figure 16: Strain failure index of the flexible aircraft (ID = 2).
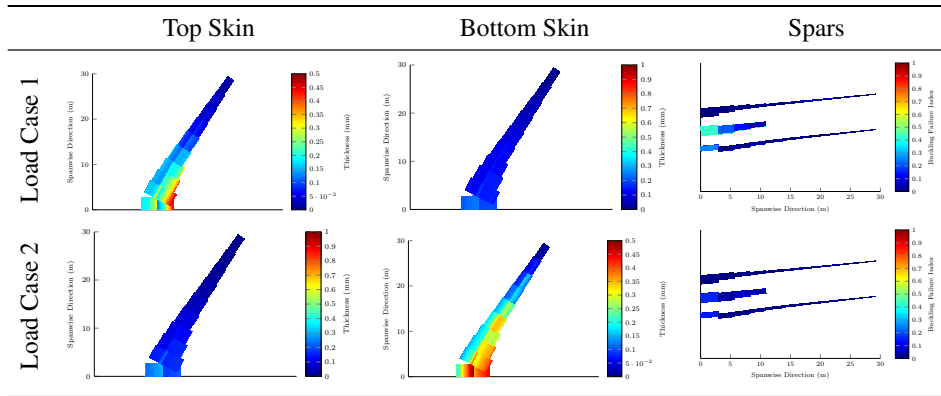
E BUCKLING FAILURE INDEX

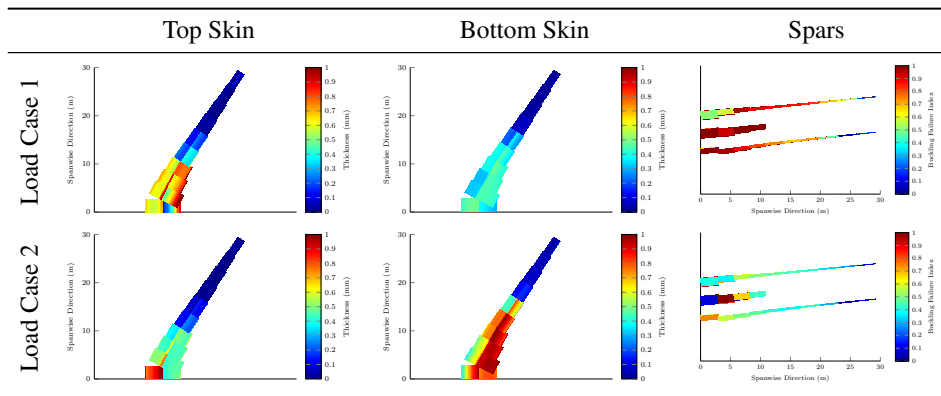Figure 17: Buckling failure index of the reference wing (ID = 0).

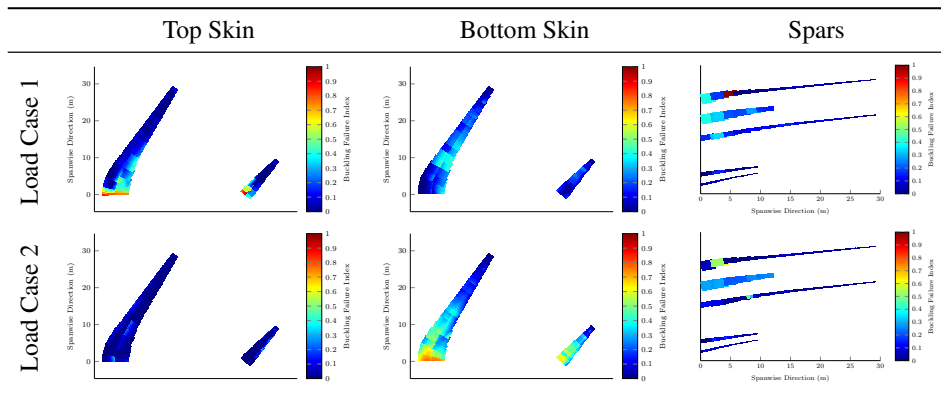Figure 18: Buckling failure index of the free-free wing (ID = 1).

Figure 19: Buckl failure index of the flexible aircraft (ID = 2).

F REFERENCES

[1] Shirk, M.H., Hertz, T.J. and Weisshaar, T.A.: Aeroelastic Tailoring - Theory, Practice and Promise, Journal of Aircraft, Vol. 23, No. 1 (1987)

[2] Weisshaar, T.A.: Aeroelastic Tailoring - Creative Use of Unusual Materials, AIAA 87-0976-CP, AIAA/ASME/ASCE/AHS 28th Structures, Structural Dynamics and Material Conference, Monterey, CA, April 6-8 (1987)

[3] Stanford, B. K., Wiesman, C. D., and Jutte, C. V.: Aeroelastic Tailoring of Transport Wings Including Transonic Flutter Constraints, 56th AIAA/ASCE/AHS/ASC Structures, Structural Dynamics, and Materials Conference, AIAA SciTech Forum, https://doi.org/10.2514/6.2015-1127, (2015)

[4] Stodieck, O., Cooper, J., Weaver, P., and Kealy, P.: Aeroelastic Tailoring of a Representative Wing-Box Using Tow-Steered Composites. AIAA Journal, DOI: 10.2514/1.J055364, (2016)

[5] Georgiou, G., Vio, G. A., and Cooper, J. E.: Aeroelastic Tailoring and Scaling Using Bacterial Foraging Optimisation. Structural and Multidisciplinary Optimization, vol. 50, no. 1, pp. 81–99. doi:10.1007/s00158-013-1033-3, (2014).

[6] Manan, A., Vio, G. A., Harmin, M. Y., and Cooper, J. E.: Optimization of aeroelastic composite structures using evolutionary algorithms. Engineering Optimization, vol. 42, no. 2, pp. 171–184. doi:10.1080/03052150903104358, (2010).

[7] Guo, S. J., Bannerjee, J. R., and Cheung, C. W.: The effect of laminate lay-up on the flutter speed of composite wings. Proceedings of the Institution of Mechanical Engineers Part G: Journal of Aerospace Engineering, vol. 217, no. 3, pp. 115–122. doi:10.1243/095441003322297225, (2003).

[8] Haddadpour, H. and Zamani, Z.: Curvilinear fiber optimization tools for aeroelastic design of composite wings. Journal of Fluids and Structures, vol. 33, pp. 180–190. doi:10.1016/j.jfluidstructs.2012.05.008, (2012).

[9] De Breuker, R., Abdalla, M.M., Gürdal, Z.: A generic morphing wing analysis and design framework, Journal of Intelligent Material Systems and Structures, vol. 22, no. 10, pp. 1025-1039 (2011)

[10] Kameyama, M. and Fukunaga, H.: Optimum design of composite plate wings for aeroelastic characteristics using lamination parameters. Computers and Structures, vol. 85, no. 3-4, pp. 213–224. doi:10.1016/J.Compstruc.2006.08.051, (2007).

[11] Jin, P., Song, B., Zhong, X., Yu, T., and Xu, F.: Aeroelastic tailoring of composite sandwich panel with lamination parameters. Proceedings of the Institution of Mechanical Engineers, Part G: Journal of Aerospace Engineering, vol. 230, no. 1. doi:10.1177/0954410015587724, (2016).

[12] IJsselmuiden, S. T.: Optimal Design of Variable Stiffness Composite Structures Using Lamination Parameters. Ph.D. thesis, Delft University of Technology, Delft, The Netherlands (2011).

[13] Khani, A., IJsselmuiden, S. T., Abdalla, M. M., and Gurdal, Z.: Design of variable stiff-ness panels for maximum strength using lamination parameters. Composites Part B: Engi-neering, vol. 42, no. 3, pp. 546–552. doi:10.1016/j.compositesb.2010.11.005 (2011).

[14] Dillinger, J. K. S., Klimmek, T., Abdalla, M. M., and Gurdal, Z.: Stiffness optimization of composite wings with aeroelastic constraints. Journal of Aircraft, vol. 50, no. 4, pp. 1159–1168. doi:10.2514/1.C032084, (2013).

[15] Dillinger, J.K.S.: Static Aeroelastic Optimization of Composite Wings with Variable Stiff-ness Laminates". PhD Dissertation, Delft University of Technology, (2014)

[16] N. Singh, S. Aikat, and B. C. Basu.: Incompressible potential flow about complete aircraft configurations. Aeronautical Journal, 93(929):335–343, (1989).

[17] Rusak, Z., Wasserstrom, E. and Seginer, A.: Numerical calculation of nonlinear aerody-namics of wing-body configurations, AIAA Journal, 21(7):929–936, (1983)

[18] Kassapoglou, C.: Design and Analysis of Composite Structures with Applications to Aerospace Structures. A John Wiley and Sons, Ltd, Publication, (2010).

[19] Battini, J.M. and Pacoste, C.: Co-rotational beam elements with warping effects in insta-bility problems, Computational Methods in Applied Mechanical Engineering, 191, 1755-1789 (2002)

[20] Gürdal, Z., Haftka, R. and Hajela, P.: Design and optimization of laminated composite materials, John Wiley and Sons, Inc (1999)

[21] Werter, N., De Breuker, R., and Abdalla, M.: Continuous-Time State-Space Unsteady Aerodynamic Modeling for Efficient Loads Analysis, AIAA Journal, 10.2514/1.J056068 (2017)

[22] Willaert, M., Abdalla, M. and Gürdal, Z.: A simple finite element cross-sectional mod-eling of thin-walled beams, Proceedings of the 2nd Aicraft Structural Design Conference (2010)

[23] Ferede, E., and Abdalla, M.: Cross-sectional modelling of thin-walled composite beams, 55th AIAA/ASME/ASCE/AHS/ASC Structures, Structural Dynamics, and Materials Con-ference, 10.2514 (2014)

[24] Werter, N., De Breuker, R.: A novel dynamic aeroelastic framework for aeroelastic tailor-ing and structural optimisation, Composite Structures, Vol. 158 - 369-386 (2016)

[25] Werter,N., De Breuker, R. and Abdalla, M.: Continuous-time stat-space unsteady aerody-namic modelling for efficient aeroelastic load analysis, International Forum on Aeroelastic-ity and Structural Dynamics, June 28 - July 2 2015, Saint Petersburg, Russia (2015)

[26] De Breuker, R., Werter. N., Dillinger, J., Meddaikar, Y. and Krüger, W., Multifidelity aeroelastic tailoring of composite wings, submitted to the CEAS journal (2017)

[27] Kassapoglou, C., "Design and Analysis of Composite Structures with Applications to Aerospace Structures". John Wiley and Sons, Ltd, Publication, (2010)

[28] Hess, J.L. and Smith, A.M.O.: Calculation of potential flow about arbitrary bodies, Progress in Aeronautical Sciences, 8:1–138, (1967)

[29] Katz, J., and Plotkin, A.: Low-Speed Aerodynamics, Mac Graw-Hill, (1991)

[30] Natella, M., Wang, X. and De Breuker, R.: The Effects of Aeroelastic Tailoring on Flight Dynamic Stability, 59th AIAA/ASCE/AHS/ASC Structures, Structural Dynamics, and Materials Conference, 2018, DOI: https://doi.org/10.2514/6.2018-0191

[31] Svanberg, K.: The method of Moving Asymptotes – A New Method for Structural Optimization. International Journal for Numerical Methods in Engineering, 24, 359-373 (1987).